Available online at www.sciencedirect.com
ScienceDirect
Chinese Journal of Natural Medicines 2020, **18**(5): 385–392
doi: 10.1016/S1875-5364(20)30045-5
Chinese Journal of Natural Medicines

•Research article•

Alkaloid constituents from the fruits of *Flueggea virosa*

XIE Qiu-Jie[1, 2Δ], ZHANG Wei-Yan[1, 2Δ], WU Zhen-Long[1, 2], XU Ming-Tao[1, 2], HE Qi-Fang[1, 2], HUANG Xiao-Jun[1, 2], CHE Chun-Tao[3], WANG Ying[1, 2*], YE Wen-Cai[1, 2*]

[1] *Institute of Traditional Chinese Medicine & Natural Products, College of Pharmacy, Jinan University, Guangzhou 510632, China;*

[2] *Guangdong Province Key Laboratory of Pharmacodynamic Constituents of TCM & New Drugs Research, Jinan University, Guangzhou 510632, China;*

[3] *Department of Pharmaceutical Sciences, College of Pharmacy, University of Illinois at Chicago, Chicago 60612, United States*

Available online 20 May, 2020

[ABSTRACT] Three new indole alkaloids, flueindolines A–C (**1**–**3**), along with nine known alkaloids (**4**–**12**), were isolated from the fruits of *Flueggea virosa* (Roxb. ex Willd.) Voigt. Compounds **1** and **2** are two new fused tricyclic indole alkaloids possessing an unusual pyrido[1, 2-a]indole framework, and **3** presents a rare spiro (pyrrolizidinyl-oxindole) backbone. Their structures with absolute configurations were elucidated by means of comprehensive spectroscopic analysis, chemical calculation, as well as *X*-ray crystallography. Chiral resolution and absolute configuration determination of the known compounds **4**, **10**, and **11** were reported for the first time. The hypothetical biogenetical pathways of **1**–**3** were herein also proposed.

[KEY WORDS] *Flueggea virosa*; Indole alkaloids; Structural elucidation; Biogenetical pathway
[CLC Number] R284 **[Document code]** A **[Article ID]** 2095-6975(2020)05-0385-08

Introduction

Flueggea virosa (Roxb. ex Willd.) Voigt. (Euphorbiaceae) is widely distributed in eastern, southern, and southwestern areas of China. Due to its cooked rice-like fruits, this plant is locally called as “Baifan Shu”. The whole plant of *F. virosa* was traditionally used as a folk medicine in China and had been proven to be effective for the treatment of rheumatism, cephalic eczema, pruritus, and injuries [1]. Previous phytochemical investigations on this plant had led to the isolation and characterization of a variety of secondary metabolites including alkaloids [2-6], terpenoids [7], bergenins [8], and flavonoids [9]. Among them, alkaloids are the best investigated group. So far, more than 70 alkaloids have been isolated and elucidated from *F. virosa*. Despite the number of alkaloids from *F. virosa* are rapidly growing in recent years, the reported alkaloids seemed to limit to a small group of indolizidine alkaloids known as *Securinega* alkaloids [10, 11].

In our continuing studies on plants of genus Flueggea [4, 5, 12-15], twelve alkaloids, including three new indole alkaloids (**1**–**3**), together with nine known alkaloids including a pyrrolidone alkaloid (**4**), two indole alkaloids (**5** and **6**), and six *β*-carboline alkaloids (**7**–**12**), were isolated from the fruits of *F. virosa* (Fig. 1). Structurally, flueindolines A (**1**) and B (**2**) are two new fused tricyclic indole alkaloids possessing an unusual pyrido[1, 2-a]indole framework, and flueindoline C (**3**) features a rare spiro (pyrrolizidinyl-oxindole) skeleton. Additionally, chiral resolution of **4**, **10**, and **11** were performed, and the absolute configurations of every pair of enantiomers were assigned for the first time. Herein, we reported the isolation, structural elucidation, and the hypothetical biogenetic pathway of these alkaloids.

Results and Discussion

Flueindoline A (**1**) was obtained as light-yellow crystals. The molecular formula of **1** was determined as $C_{13}H_{14}N_2O_2$ on the basis of its HR-ESI-MS data (*m/z* 231.1145 $[M + H]^+$, Calcd. for $C_{13}H_{15}N_2O_2$ 231.1128). The UV bands at 216, 250,

[Received on] 15-Dec.-2019
[Research funding] This work was supported by the National Key R & D Program of China (No. 2018YFC1706200), the National Natural Science Foundation of China (Nos. 81630095, 81622045, and 81803379), the Science & Technology Program of China (No. 2019ZX09735002-003), the China Postdoctoral Science Foundation (Nos. 2019T120794, and 2018M633291), and the Local Innovative and Research Teams Project of Guangdong Pearl River Talents Program (No. 2017BT01Y036).
[*Corresponding author] Tel: 86-20-85223553, E-mail: wangying_cpu@163.com (WANG Ying); Tel: 86-20-85220936, E-mail: chywc@aliyun.com (YE Wen-Cai)
[Δ]These authors contributed equally to this work.
These authors have no conflict of interest to declare.

and 294 nm as well as the IR absorptions at 3503, 3346, 1625, and 1577 cm^{-1} indicated the existence of hydroxy, amide group, and aromatic ring in **1**. In the ^{1}H NMR spectrum of **1**, characteristic signals corresponding to a 1,2,4-trisubstituted benzene ring [δ_H 7.24 (d, J = 2.0 Hz, H-4), 7.20 (d, J = 8.7 Hz, H-7), and 6.73 (dd, J = 8.7, 2.0 Hz, H-6)] and four methylenes [δ_H 4.05 (2H, t, J = 6.0 Hz, H_2-11), 3.21 (2H, t, J = 6.0 Hz, H_2-8), 2.09 (2H, m, H_2-10), and 1.92 (2H, m, H_2-9)] were observed. The ^{13}C NMR spectrum of **1** revealed the presence of thirteen carbon signals, which were assigned under the assistance of DEPT-135 spectrum to a carbonyl group [δ_C 171.4 (C-12)], eight aromatic and olefinic carbons [δ_C 153.7 (C-5), 144.3 (C-2), 132.4 (C-7a), 128.1 (C-3a), 112.0 (C-6), 110.8 (C-7), 105.7 (C-3), and 105.3 (C-4)], and four methylene carbons. Based on the comprehensive analysis of ^{1}H–^{1}H COSY, HSQC, and HMBC spectra, the ^{1}H and ^{13}C NMR spectral data of **1** were assigned and shown in Table 1.

The ^{1}H-^{1}H COSY spectrum of **1** displayed the presence of two spin-coupling systems (H-6 to H-7 and H_2-8 to H_2-11). In the HMBC spectrum, correlations between H-4 and C-3/C-6/C-7a, between H-6 and C-7a, as well as between H-7 and C-5/C-3a established an indole fragment, in which C-5 was oxygenated due to its obvious downfield shift (δ_C 153.7). Furthermore, HMBC correlations between H_2-8 and C-3, between H_2-9 and C-2, and between H_2-11 and C-2/C-7a indicated that a C4 unit was fused to the indole motif through N-1 and C-2. Therefore, the tetrahydropyrido[1,2-a]indole core skeleton of **1** was established. Moreover, the remaining carbonyl and amino groups could be assigned to a carboxamide moiety on the basis of molecular formula information. Considering the obvious upfield shift of C-3 (δ_C 105.7), the carboxamide moiety was determined to link to C-3 position of the tetrahydropyrido[1,2-a]indole core (Fig. 2). Finally, the

Table 1 ^{1}H (500 MHz) and ^{13}C (125 MHz) NMR spectroscopic data of 1 and 2 in CD_3OD

No.	1		2	
	δ_H	δ_C	δ_H	δ_C
2	–	144.3	3.37, td (10.6, 2.5)	70.0
3	–	105.7	3.56, d (10.6)	55.1
3a	–	128.1	–	129.2
4	7.24, d (2.0)	105.3	7.06, overlapped	124.7
5	–	153.7	6.65, td (8.0, 1.0)	119.3
6	6.73, dd (8.7, 2.0)	112.0	7.06, overlapped	129.4
7	7.20, d (8.7)	110.8	6.50, d (8.0)	107.7
7a	–	132.4	–	152.8
8	3.21, t (6.0), 2H	25.4	α 1.54, dd (13.5, 4.0)	30.9
			β 1.90, overlapped	
9	1.92, m, 2H	21.3	α 1.91, overlapped	25.4
			β 1.47, m	
10	2.09, m, 2H	23.7	α 1.61, m	25.8
			β 1.76, m	
11	4.05, t (6.0), 2H	43.6	α 3.66, dd (12.0, 5.0)	46.6
			β 2.61, td (12.0, 3.0)	
12		171.4	–	177.2

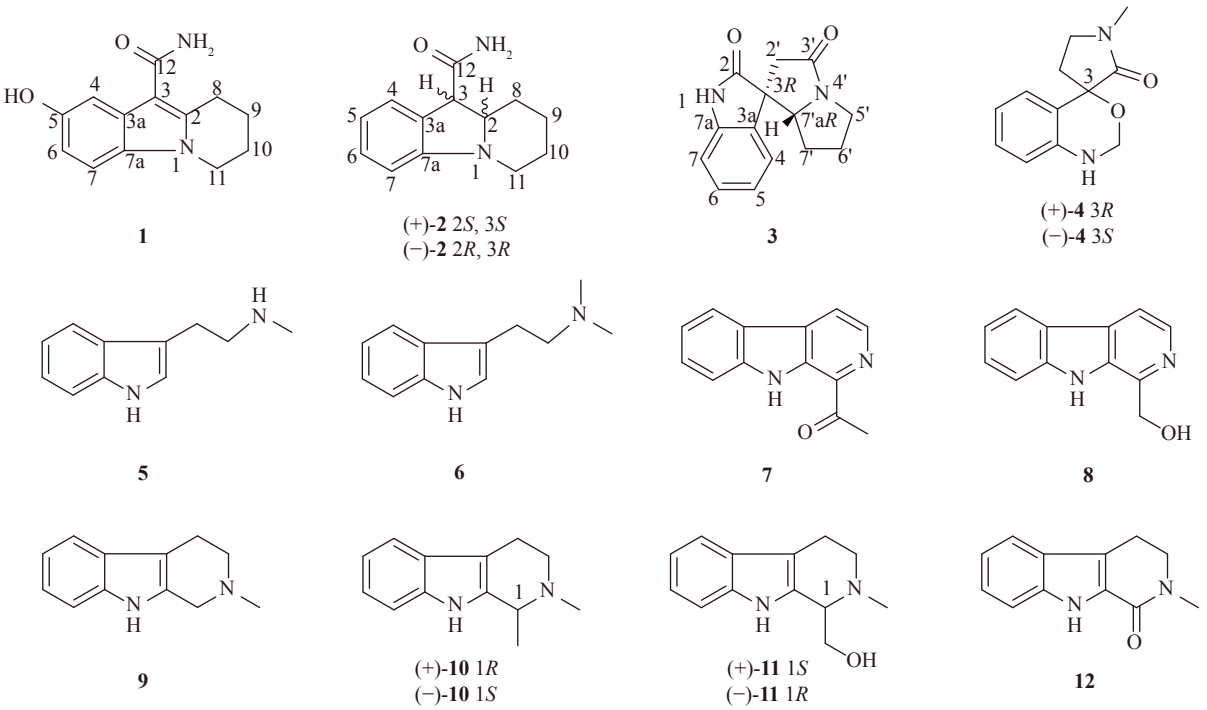

Fig. 1 Chemical structures of 1–12

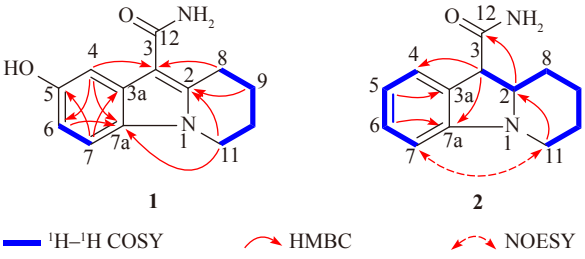

Fig. 2 Key 2D NMR correlations of 1 and 2

structure of **1** was confirmed by a following single crystal X-ray diffraction experiment (Fig. 3).

Flueindoline B (**2**) was isolated as pale-yellow oil. Its molecular formula was established as $C_{13}H_{16}N_2O$ by its HR-ESI-MS at *m/z* 217.1333 $[M + H]^+$ (Calcd. for $C_{13}H_{17}N_2O$: 217.1335). The UV spectrum of **2** showed the absorption maxima at 207, 254, and 297 nm. The IR spectrum presented the characteristic absorptions for amide group (3376 and 1652 cm^{-1}) and aromatic ring (1597, 1581, and 1451 cm^{-1}). Similar to **1**, the ^{1}H and ^{13}C NMR spectra of **2** displayed characteristic signals for a substituted benzene ring, a carboxamide, and four methylenes, suggesting the structural similarity of these two compounds. Different from **1**, the NMR spectra of **2** showed the presence of an *ortho*-disubstituted benzene ring [δ_H 7.06 (2H, overlapped, H-4 and H-6), 6.65 (td, J = 8.0, 1.0 Hz, H-5), and 6.50 (d, J = 8.0 Hz, H-7); δ_C 152.8 (C-7a), 129.4 (C-6), 129.2 (C-3a), 124.7 (C-4), 119.3 (C-5), and 107.7 (C-7)]. Moreover, the signals corresponding to a tetrasubstituted double bond in **1** were replaced by signals of two methine groups [δ_H 3.56 (d, J = 10.6 Hz, H-3) and 3.37 (td, J = 10.6, 2.5 Hz, H-2); δ_C 70.0 (C-2) and 55.1 (C-3)] in **2**. The above spectroscopic data suggested that **2** was a C-5 dehydroxylated and $\Delta^{2,3}$ double bond hydrogenated derivative of **1**. With the aid of ^{1}H–^{1}H COSY, HSQC, and HMBC spectra, the ^{1}H and ^{13}C NMR spectral data of **2** were assigned (Table 1).

The ^{1}H–^{1}H COSY spectrum of **2** showed the existence of two spin-coupling systems (H-3 to H_2-11 and H-4 to H-7), suggesting the presence of a hexahydropyrido[1, 2-a]indole core in **2**. The above result was further confirmed by HMBC correlations between H-3 and C-4/C-7a, between H-5 and C-3a, between H-6 and C-7a, and between H-11α and C-2. This assignment was also supported by the NOE correlation between H-7 and H-11α. Furthermore, a carboxamide moiety was assigned to attach to C-3 position of the hexahydropyrido[1, 2-a]indole core on the basis of HMBC correlation between H-2 and C-12. Hence, the planar structure of **2** was established as shown in Fig. 2.

To establish the relative configuration of **2**, the theoretical ^{1}H and ^{13}C NMR data of its two possible C-2 and C-3 stereoisomers, 2S^*, 3S^*-**2** and 2S^*, 3R^*-**2**, were calculated using the GIAO method at mPW1PW91/6-311G(d,p) level in methanol solution [16]. The experimental and calculated ^{13}C NMR chemical shifts were subsequently analyzed by employing the DP4$^+$ method [17]. With DP4$^+$ probabilities of 100% and 0% for 2*S**, 3*S**-**2** and 2*S**,3*R**-**2**, respectively, the relative configuration of **2** could be determined to 2*S**, 3*S**. Additionally, the torsion angle of H-2–C-2–C-3–H-3 ($\phi_{H2\text{-}C2\text{-}C3\text{-}H3}$) was 37.8° in the conformation optimized structure of 2*S**, 3*S**-**2**, which was consistent with the observed vicinal proton-proton coupling constant of H-2 and H-3 ($^3J_{H\text{-}2,H\text{-}3}$ = 10.6 Hz) in the ^{1}H NMR spectrum of **2** (Fig. 4).

Although there are two asymmetric carbons in the molecule of **2**, its optical rotation value was very close to zero, suggesting the presence of a racemic mixture of **2**. Subsequently, **2** was resolved into two enantiomers, (+)-**2** and (−)-**2**, at a ratio of 1 : 1 on a Phenomenex Lux® cellulose-2 column. The ECD spectra of (+)-**2** and (−)-**2** displayed similar signal intensities but opposite Cotton effects, confirming their enantiomeric relationship. The absolute configurations of the two enantiomers were further determined by comparison of their experimental ECD spectra with those predicted by time-dependent density functional theory (TDDFT) calculation at the PCM(MeOH)/ωB97XD/aug-cc-pVDZ level. As shown in Fig. 5, the calculated ECD curves of 2*S*,3*S*-**2** and 2*R*,3*R*-**2** displayed good agreement with the experimental values of (+)-**2** and (−)-**2**, respectively. Therefore, the absolute configurations of (+)-**2** and (−)-**2** were respectively elucidated as 2*S*, 3*S* and 2*R*, 3*R*.

The molecular formula of flueindoline C (**3**) was assigned as $C_{14}H_{14}N_2O_2$ by its HR-ESI-MS (*m/z* 243.1127 $[M + H]^+$, calcd. for $C_{14}H_{15}N_2O_2$ 243.1128). The UV spectrum showed the absorption maxima at 210 and 256 nm. The IR spectrum displayed the presence of amide group (3413 and 1658 cm^{-1}) and benzene ring (1604 and 1484 cm^{-1}) in **3**. The

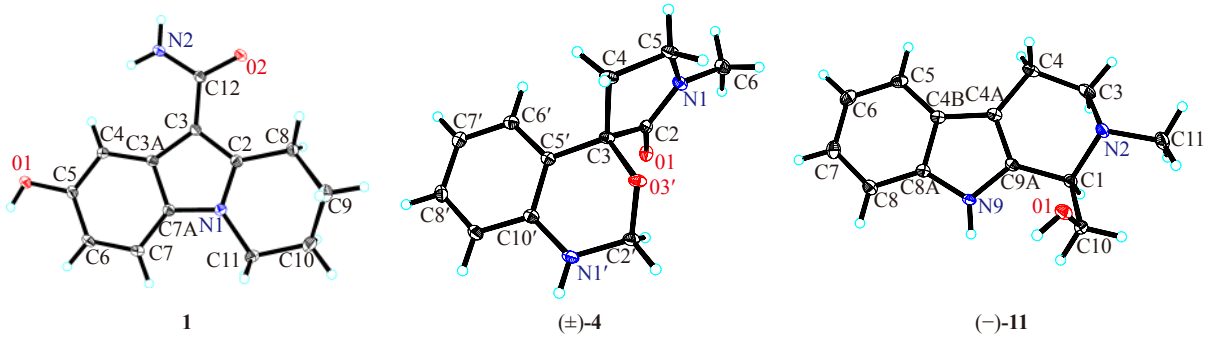

Fig. 3 X-ray ORTEP drawings of 1, (±)-4, and (−)-11

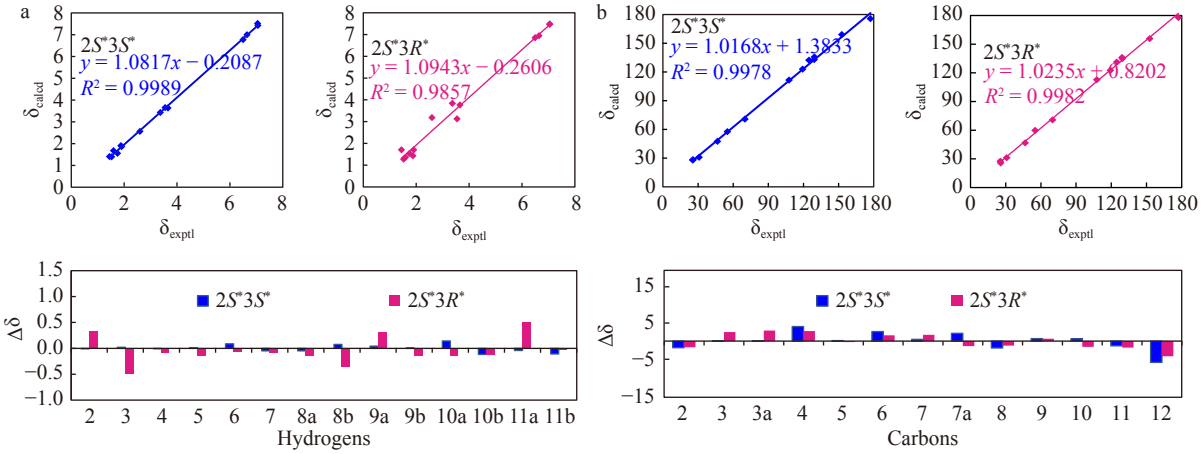

Fig. 4 Calculated ^{1}H and ^{13}C NMR chemical shifts of the two possible isomers of 2 at the mPW1PW91/6-311G(d,p) level. (a) Linear correlation plots and the relative errors between the calculated ^{1}H chemical shifts of two potential structures and the experimental ^{1}H NMR data of 2. (b) Linear correlation plots and the relative errors between the calculated ^{13}C chemical shifts of two potential structures and the experimental ^{13}C NMR data of 2

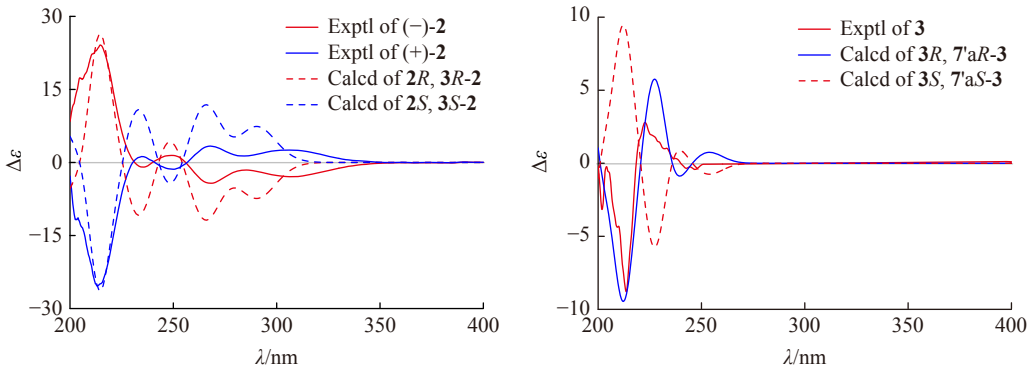

Fig. 5 Calculated and experimental ECD spectra of 2 (left) and 3 (right)

^{1}H NMR spectrum of **3** revealed resonances for an *ortho*-disubstituted benzene ring [δ_H 7.28 (dd, J = 7.5, 1.4 Hz, H-6), 7.11 (d, J = 7.5 Hz, H-4), 7.05 (td, J = 7.5, 1.0 Hz, H-5), and 6.92 (d, J = 7.5 Hz, H-7)]. The ^{13}C NMR spectrum exhibited fourteen carbon signals including two carbonyl carbons, six aromatic carbons, a quaternary carbon, a methine carbon, and four methylene carbons. With the aid of ^{1}H–^{1}H COSY, HSQC, and HMBC experiments, the ^{1}H and ^{13}C NMR signals of **3** were assigned as shown in Table 2.

Interpretation of the ^{1}H–^{1}H COSY correlations led to the assignment of two spin-coupling systems (H-4 to H-7 and H_2-5′ to H-7′a) in **3**. In the HMBC spectrum of **3**, correlations between H-4 and C-3/C-7a, and between H-7 and C-3a allowed the establishment of an oxindole moiety (**3a**). Meanwhile, the HMBC correlations between H_2-5′ and C-7′a/C-3′, between H-2′b and C-7′a, as well as between H_2-7′ and C-3 suggested the presence of an oxipyrrolizidine moiety (**3b**) in **3**. Furthermore, the HMBC cross peaks between H-7′a and C-2/C-3a, and between H_2-2′ and C-2/C-3a indicated that the two fragments **3a** and **3b** were connected by sharing the same quaternary carbon C-3, resulting the formation of a spiro[pyrrolizidine-1,3-oxindoline] scaffold (Fig. 6).

The NOESY spectrum of **3** exhibited NOE correlations between H-7′a and H-2′*β*/H-5′*β*/H-7′*β*, indicating that these protons were cofacial in the pyrrolizidine moiety. Furthermore, the NOE correlations between H-4 and H-2′*α*/H-7′*α* suggested that these protons located in the same orientation of the molecule. Therefore, based on the above spectroscopic data, the relative configuration of **3** could be assigned as 3*R**, 7′a*R** (Fig. 6). To determine the absolute configuration, the theoretical ECD spectra of two possible stereoisomers of **3**, 3*R*, 7′a*R*-**3** and 3*S*, 7′a*S*-**3**, were predicted by TDDFT calculation. As a result, the calculated ECD curve of isomer 3*R*,7′a*R*-**3** revealed a good agreement with the experimental one (Fig. 5). Therefore, the absolute configuration of **3** was assigned as 3*R*,7′a*R*.

Compound **4** was obtained as light-yellow needles. Based on comparison of the UV, IR, MS, as well as NMR data with the literature [18], **4** was identified as the known compound donaxanine. Fortunately, suitable crystals of **4** for X-ray crystallographic analysis were successfully obtained in this study. Thus, the structure of donaxanine (**4**) was unambiguously substantiated (Fig. 3). In the initial literature, neither the optical rotation value nor the stereostructure of

Table 2 ^{1}H (600 MHz) and ^{13}C (150 MHz) NMR spectroscopic data of 3 in $CDCl_3$

No.	δ_H	δ_C
2	–	178.0
3	–	54.1
3a	–	130.2
4	7.11, d (7.5)	123.8
5	7.05, td (7.5, 1.0)	122.9
6	7.28, dd (7.5, 1.4)	129.0
7	6.92, d (7.5)	110.2
7a	–	139.7
2′	*α* 2.52, d (15.6) *β* 3.47, d (15.6)	45.6
3′	–	170.9
5′	*α* 3.68, m *β* 3.17, m	41.3
6′	2.04, m, 2H	27.0
7′	*α* 1.31, dd (12.6, 8.4) *β* 1.61, m	25.2
7′a	4.40, t (7.8)	67.7

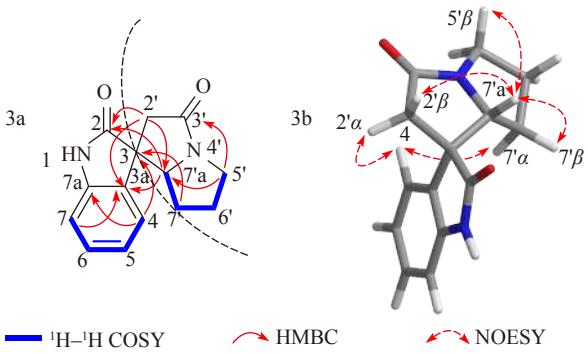

Fig. 6 Key 2D NMR correlations of 3

donaxanine was mentioned. Interestingly, the crystal structure of **4** showed a centrosymmetric space group of $P2_1/c$, together with its barely measurable optical rotation value, indicating that **4** was obtained as a racemic mixture in this study. Furthermore, **4** was resolved into two enantiomers, (+)-**4** ($[\alpha]_D^{25}$ +28.1) and (−)-**4** ($[\alpha]_D^{25}$ −26.6), on a Phenomenex Lux® cellulose-2 column. Similar to **2**, the absolute configurations of (+)-**4** and (−)-**4** were finally established as 3*R* and 3*S*, respectively, by TDDFT ECD calculation (Fig. 7).

Compound **10** was identified as N_b-methyltetrahydroharman on the basis of the comparison of its spectrocopic data with those of the known compound [19]. In the literature, N_b-methyltetrahydroharman was reported to possess a positive specific rotation value ($[\alpha]_D^{25}$ +26), and the stereochemistry of C-1 was determined as *R*. However, in this study **10** was obtained as a racemate ($[\alpha]_D^{25}$ ±0). Further chiral resolution of **10** gave a pair of enantiomers (+)-**10** ($[\alpha]_D^{25}$ +15.7) and (−)-**10** ($[\alpha]_D^{25}$ −18.3), and their absolute configurations were subsequently determined as 1*R* and 1*S* by TDDFT ECD calculation (Fig. 7).

Compound **11** showed identical ^{1}H and ^{13}C NMR spectral data to those of 1-hydromethyl-2-methyl-tetrahydro-*β*-carboline [20] Although there was an asymmetric carbon in the molecule of 1-hydromethyl-2-methyl-tetrahydro-*β*-carboline, the original literature did not report its optical rotation value and absolute configuration. In current study, **11** was also isolated as a racemic mixture which was further resolved into a pair of enantiomers, (+)-**11** ($[\alpha]_D^{25}$ +15.0) and (−)-**11** ($[\alpha]_D^{25}$ −13.8). Subsequently, the absolute configuration of (−)-**11** was determined as 1*R* [Cu Kα, Flack parameter = −0.02(12), Fig. 3 by single-crystal *X*-ray diffraction analysis. Moreover, the absolute configurations of (+)-**11** and (−)-**11** were further confirmed to be 1*S* and 1*R*, respectively, by comparing their experimental and calculated ECD spectra (Fig. 7).

The remaining six known alkaloids were identified as methyltryptamine (**5**) [21], *N*, *N*-dimethyltryptamine (**6**) [22], 1-acetyl-*β*-carboline (**7**) [23], 1-hydroxymethyl-*β*-carboline (**8**) [24], *N*-methyl-1, 2, 3, 4-tetrahydro-*β*-carboline (**9**) [25], and strychnocarpine (**12**) [26], repectively, by comparison of their spectroscopic data with reported ones.

Compounds **1**–**3** are three novel indole alkaloids with rare architectures. Their hypothetical biogenetic pathways were proposed as outlined in Scheme 1, which utilized tryptophan, acetyl-CoA, and ornithine as the biogenetic precursors. Briefly, enzymatic decarboxylation and oxidation of the putative precursor tryptophan could result in the generation of indoleacetic acid and indole-3-carboxamide. On the one

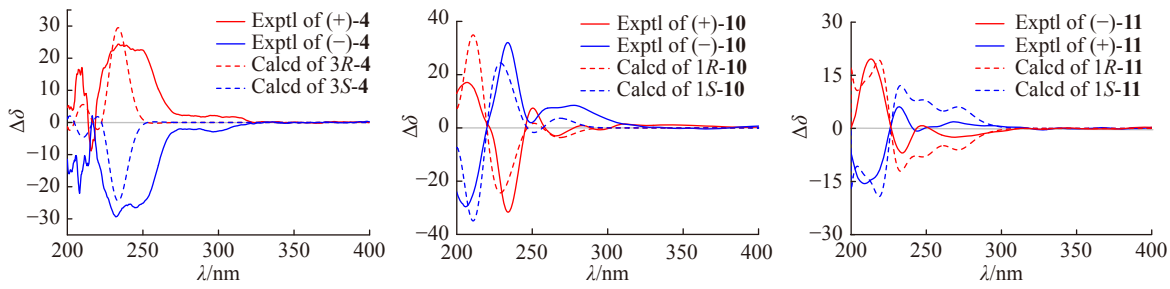

Fig. 7 Calculated and experimental ECD spectra of 4, 10, and 11

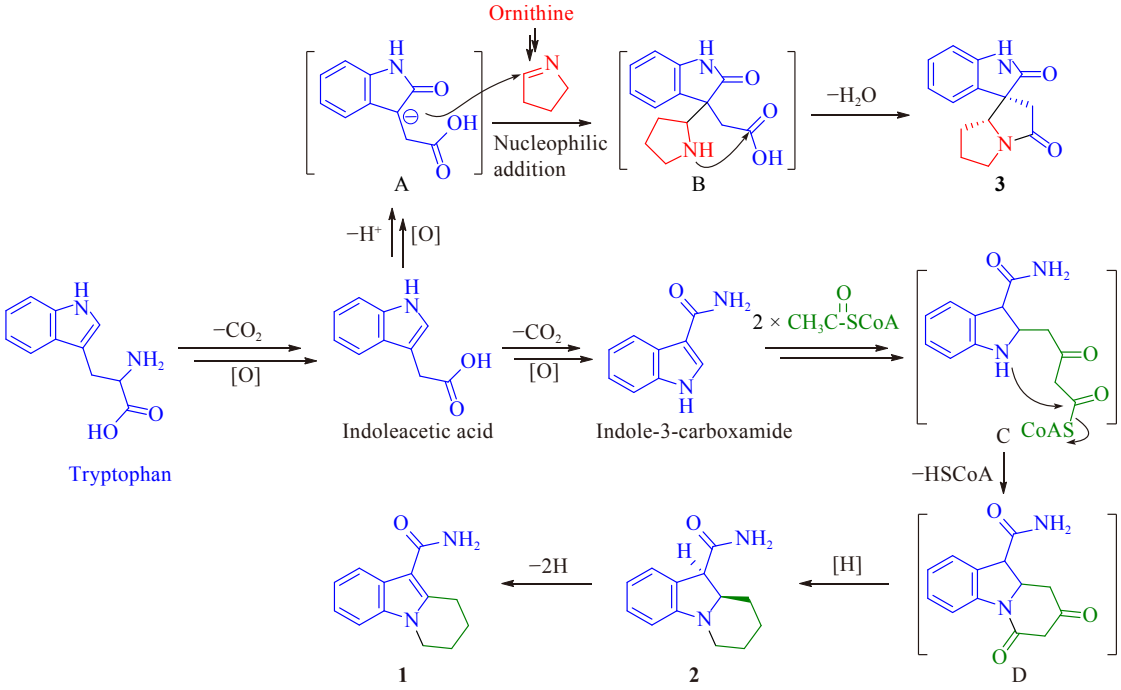

Scheme 1 Hypothetical biogenetic pathways for 1–3

hand, oxidation and deprotonation of indoleacetic acid could lead to the formation of oxindole intermediate **A**. After an intermolecular nucleophilic addition between **A** and Δ^1-pyrrole, which could be derived from amino acid precursor ornithine, the pyrrole unit was assembled to the C-3 position of the indole core and yielded intermediate **B**. Subsequently, intramolecular nucleophilic addition and hydrolysis of **B** could generate **3**. On the other hand, indole-3-carboxamide could couple with two molecules of acetyl-CoA at the C-2 position of the indole core successively, resulting in the side chain extension of indole-3-carboxamide at C-2 position and the formation of intermediate **C**. Similar to the transformation from intermediate **B** to **3**, intermediate **C** could give intermediate **D** through an intramolecular ring-closure reaction. Finally, compounds **1** and **2** could be formed via the successive reduction and dehydrogenation processes of intermediate **D**. It is worth mentioning that alkaloids isolated from genus Fluggea commonly belonged to *Securinega* alkaloids, which were proved to be originated from amino acid precursors lysine, tyrosine, and ornithine. In this study, the discovery of a series of indole, pyrrolidone, and β-carboline alkaloids from *F. virosa* illustrated the participation of other biogenetic precursors in alkaloids biosynthesis in this genus.

Previous studies demonstrated that many indole and *β*-carboline alkaloids exhibited significant neuroprotective and antiviral activities [27,28]. Accordingly, all isolated alkaloids were evaluated for their neuroprotective activities on Neural-2a cells and anti-virus effects against the respiratory syncytial virus (RSV), respectively. However, none of the tested compounds exhibited significant activities at the tested concentration (50 μmol·L^{-1}).

In summary, two new fused tricyclic indole alkaloids (**1** and **2**) and a new spirooxindole alkaloid (**3**), together with nine known alkaloids (**4**–**12**) were isolated and identified from the fruits of *Flueggea virosa* (Roxb. ex Willd.) Voigt. Their structures with absolute configurations were elucidated by comprehensive spectroscopic analysis, computation, as well as X-ray diffraction. The discovery of **1**–**12** demonstrated that tryptophan was invloved in the alkaloids biosynthesis in the *Flueggea* genus besides the common precursors tyrosine, lysine, and ornithine, suggesting the potential structural diversity of alkaloid constituents in this plant genus.

Experimental

General experimental procedures

Optical rotations were measured on a Jasco P-1020 digital polarimeter (Jasco, Tokyo, Japan) with a 1 cm cell at room temperature. UV spectra were recorded on a JASCO V-550 UV/VIS spectrophotometer with a 1 cm length cell. IR spectra were obtained on a JASCO FT/IR-480 plus Fourier Transform infrared spectrometer (KBr pellets). ECD spectra were recorded on a Jasco J-810 spectropolarimeter at room temperature. HR-ESI-MS were acquired from an Agilent 6210 LC/MSD TOF mass spectrometer equipped with ESI source. 1D and 2D NMR spectra were recorded on a Bruker AV-500 spectrometer (^{1}H: 500 MHz, ^{13}C: 125 MHz) and a Bruker AV-600 spectrometer (^{1}H: 600 MHz, ^{13}C: 150 MHz). TLC analyses were carried out using precoated silica gel GF_{254} plates (Qingdao Marine Chemical Plant, Qingdao, China). Column chromatographies were performed on silica gel (200–300 mesh, Qingdao Marine Chemical Plant, Qingdao, China) and Sephadex LH-20 (Pharmacia Uppsala, Sweden). Analytical HPLC and preparative HPLC were carried out on Agilent 1260 instruments equipped with MWD detectors

(Agilent 1260, MWDVL, USA) and XBridge® C18 column (i.d. 4.6 and 19 mm × 250 mm, 5 μm, Waters, Ireland). All solvents used in column chromatography and HPLC were of analytical grade (Damao Chemical Plant, Tianjin, China) and chromatographic grade (Fisher Scientific, New Jersey, USA), respectively.

Plant materials

The ripe fruits of *Flueggea virosa* were collected from Guilin city, Guangxi Autonomous Region of China, in October of 2014, and authenticated by Prof. ZHOU Guang-Xiong (Jinan University). A voucher specimen (No. 20141018-1) was deposited in the Institute of Traditional Chinese Medicine & Natural Products, Jinan University, Guangzhou, China.

Extraction and isolation

The air-dried and powdered material (50 kg) was percolated with 95% (*V*/*V*) EtOH at room temperature to give 10.0 kg of crude extract, which was suspended in H_2O and acidified with 10% HCl to pH 3. After removal of the neutral components by using $CHCl_3$ as a solution, the aqueous layer was then basified with NH_4OH to pH 9 and re-extracted with $CHCl_3$ to obtain the total alkaloid fraction (63 g). The alkaloid fraction was subjected to silica gel column ($CHCl_3$-CH_3OH, 100 : 0→0 : 100, *V*/*V*) to give ten major fractions (Fr. 1–Fr. 10). Fr. 2 was re-subjected to a silica gel column, and then purified with preparative HPLC to give **3** (2.0 mg). Fr. 6 was loaded to a Sephadex LH-20 column to afford five sub-fractions (Fr. 6A–Fr. 6E). Fr. 6B was subsequently subjected to silica gel column and purified with preparative HPLC to give **4** (2.3 mg), **5** (5.6 mg), and **6** (16.0 mg). Fr. 6C was also purified by preparative HPLC to give **7** (2.9 mg) and **12** (6.2 mg). Fr. 7 was subjected to a silica gel column to afford sub-fractions Fr. 7A–Fr. 7G. Then, Fr. 7B was reloaded to a Sephadex LH-20 column and purified by preparative HPLC to yield **9** (27.9 mg) and **10** (15.6 mg). Fr. 7D was purified by preparative HPLC to give **11** (18.0 mg). Fr. 7E was further purified by a silica gel column and preparative HPLC to give **1** (2.8 mg), **2** (3.0 mg), and **8** (2.0 mg).

Enantioseparations of (±)-**2**, (±)-**4**, (±)-**10**, and (±)-**11** were carried out on an Agilent 1260 liquid chromatograph system equipped with a DAD detector. As a result, (+)-**2** (t_R 4.7 min, 1.3 mg) and (−)-**2** (t_R 5.2 min, 1.3 mg), (+)-**4** (t_R 5.2 min, 1.0 mg) and (−)-**4** (t_R 5.6 min, 1.0 mg), (+)-**10** (t_R 5.3 min, 7.0 mg) and (−)-**10** (t_R 5.0 min, 7.0 mg), as well as (+)-**11** (t_R 4.5 min, 8.5 mg) and (−)-**11** (t_R 5.0 min, 8.5 mg) were obtained by using a Phenomenex Cellulose-2 column (i.d. 4.6 mm × 250 mm, 5 μm, Phenomenex, CA, USA) and an elution mixture of MeOH−H_2O (80 : 20) at a flow rate of 1 mL·min^{-1}, respectively.

*Flueindoline A (**1**)*

Light-yellow crystals (CH_3OH-$CHCl_3$); UV (CH_3OH) λ_{max} 216, 250, and 294 nm; IR (KBr) ν_{max} 3503, 3346, 1625, 1577, 1519, 1455, 1371, and 1213 cm^{-1}; HR-ESI-MS *m*/*z* 231.1145 $[M + H]^+$ (Calcd. for $C_{13}H_{15}N_2O_2$: 231.1128). For ^1H and ^{13}C NMR spectral data: see Table 1.

*(±)-Flueindoline B [(±)-**2**]*

Pale yellow oil (CH_3OH); $[\alpha]_D^{25}$ ±0 (*c* 0.1, CH_3OH); UV (CH_3OH) λ_{max} 207, 254, and 297 nm; IR (KBr) ν_{max} 3376, 1652, 1597, 1581, 1451, 1382, 1249, and 1066 cm^{-1}; HR-ESI-MS *m*/*z* 217.1333 $[M + H]^+$ (Calcd. for $C_{13}H_{17}N_2O$: 217.1335). For ^1H and ^{13}C NMR spectral data: see Table 1.

(+)-**2**: pale yellow oil; $[\alpha]_D^{25}$ +37.7 (*c* 1.0, CH_3OH); ECD (CH_3OH) λ_{max} (Δε) 215 (−24.6), 235 (+1.21), 250 (−1.39), 267 (+3.36), and 308 (+2.53).

(−)-**2**: pale yellow oil; $[\alpha]_D^{25}$ −35.6 (*c* 1.0, CH_3OH); ECD (CH_3OH) λ_{max} (Δε) 216 (+23.4), 235 (−0.95), 249 (+1.44), 268 (−4.27), and 307 (−2.93).

*Flueindoline C (**3**)*

Pale-yellow oil (CH_3OH); $[\alpha]_D^{25}$ +18.6 (*c* 1.0, CH_3OH); UV (CH_3OH) λ_{max} 210 and 256 nm; IR (KBr) ν_{max} 3413, 1658, 1604, 1484, and 1400 cm^{-1}; HR-ESI-MS *m*/*z* 243.1127 $[M + H]^+$ (Calcd. for $C_{14}H_{15}N_2O_2$: 243.1128). ECD (CH_3OH) λ_{max} (Δε) 214 (−8.79), 223 (+2.78), and 247 (−0.43). For ^1H and ^{13}C NMR spectral data: see Table 2.

*X-ray crystallographic analysis of **1***

$C_{13}H_{14}N_2O_2$ (*M* = 230.26 g·mol^{-1}): monoclinic, space group $P2_1/c$ (no. 14), *a* = 8.322 30(10) Å, *b* = 7.465 50(10) Å, *c* = 17.7704(3) Å, *β* = 100.6380(10), *V* = 1085.10(3) Å^3, *Z* = 4, *T* = 100.00(10) K, μ(Cu Kα) = 0.786 mm^{-1}, *Dcalc* = 1.409 g·cm^{-3}, 8170 reflections measured (10.13° ≤ 2Θ ≤ 147.492°), 2168 unique (R_{int} = 0.0259, R_{sigma} = 0.0174) which were used in all calculations. The final R_1 was 0.0428 (I > 2σ(I)) and wR_2 was 0.1117 (all data). Crystallographic data for the structure of **1** have been deposited in the Cambridge Crystallographic Data Centre (deposition number: CDCC 1 957 483).

*X-ray crystallographic analysis of (±)-**4***

$C_{12}H_{14}N_2O_2$ (*M* =218.26 g·mol^{-1}): monoclinic, space group $P2_1/c$ (no. 14), *a* = 7.113 48(12) Å, *b* = 9.574 95(13) Å, *c* = 15.6174(2) Å, *β* = 92.5337(14)°, *V* = 1062.68(3) Å^3, *Z* = 4, *T* = 100.00(10) K, μ(Cu Kα) = 0.769 mm^{-1}, *Dcalc* = 1.3641 g·cm^{-3}, 19788 reflections measured (10.84° ≤ 2Θ ≤ 147.38°), 2127 unique (R_{int} = 0.0331, R_{sigma} = 0.0137) which were used in all calculations. The final R_1 was 0.0352 (I ≥ 2μ(I)) and wR_2 was 0.0929 (all data). Crystallographic data for the structure of (±)-**4** have been deposited in the Cambridge Crystallographic Data Centre (deposition number: CDCC 1 957 484).

*X-ray crystallographic analysis of (−)-**11***

$C_{13}H_{16}N_2O$ (*M* =216.28 g·mol^{-1}): orthorhombic, space group $P2_12_12_1$ (no. 19), *a* = 6.810 40(10) Å, *b* = 7.502 10(10) Å, *c* = 22.2786(3) Å, *V* = 1138.26(3) Å^3, *Z* = 4, *T* = 100.00(10) K, μ(Cu Kα) = 0.643 mm^{-1}, *Dcalc* = 1.2620 g·cm^{-3}, 10765 reflections measured (7.936° ≤ 2Θ ≤ 147.85°), 2265 unique (R_{int} = 0.0324, R_{sigma} = 0.0239) which were used in all calculations. The final R_1 was 0.0329 (I ≥ 2μ(I)) and wR_2 was 0.0807 (all data). Crystallographic data for the structure of (−)-**11** have been deposited in the Cambridge Crystallographic Data Centre (deposition number: CDCC 1 957 485).

Computational methods

The random search program with MMFF94S force field

in Sybyl-X 2.1.1 package was invoked for conformational search of the possible isomers of **2** (2*S*,3*S*-**2** and 2*S*,3*R*-**2**). Only one conformer was obtained for each of the two isomers. These two conformers were optimized and applied for the NMR chemical shifts calculation by using the DFT method at the mPW1PW91/6-311G(d,p) level in methanol (PCM) in Gaussian 09 software [29]. The calculated ^{1}H and ^{13}C shielding tensors were statistically analyzed with the experimental ones by using linear regression and DP4^{+} probability. The ECD data of 2*S*,3*S*-**2** was calculated with the TD/ωB97XD/aug-cc-pVDZ methods in methonal and compared to the experimental ones in SpecDis 1.71 software [30]. Conformational analysis of the plausible stereoisomers of compounds **3**, **4**, **10**, and **11** was performed by using a similar method to **2**. The predicted ECD curves of the selected conformers of 3*R*, 7′a*R*-**3**, 3*R*-**4**, 1*R*-**10**, and 1*R*-**11** were calculated with the TD/B3LYP/6-31 + G(d) method in methanol in Gaussian 09 software, and analyzed in SpecDis 1.71 software, respectively.

References

[1] Editorial Committee of Flora of China. *Flora of China* [M]. Beijing: Science Press, 1997: 69−71.

[2] Luo XK, Cai J, Yin ZY, *et al*. Fluvirosaones A and B, two indolizidine alkaloids with a pentacyclic skeleton from *Flueggea virosa* [J]. *Org Lett*, 2018, **20**(4): 991–994.

[3] Zhang H, Zhu KK. Gao XH, *et al*. Natural occurrence of all eight stereoisomers of a neosecurinane structure from *Flueggea virosa* [J]. *Tetrahedron*, 2017, **73**(31): 4692–4697.

[4] Zhao BX, Wang Y, Zhang DM, *et al*. Virosaines A and B, two new birdcage-shaped Securinega alkaloids with an unprecedented skeleton from *Flueggea virosa* [J]. *Org Lett*, 2012, **14**(12): 3096–3099.

[5] Zhao BX, Wang Y, Zhang DM, *et al*. Flueggines A and B, two new dimeric indolizidine alkaloids from *Flueggea virosa* [J]. *Org Lett*, 2011, **13**(15): 3888–3891.

[6] Yang X, Liu J, Huo Z, *et al*. Fluevirines E and F, two new alkaloids from *Flueggea virosa* [J]. *Nat Prod Res*, 2019.

[7] Wang XF, Liu FF, Zhu Z, *et al*. Flueggenoids A-E, new dinorditerpenoids from *Flueggea virosa* [J]. *Fitoterapia*, 2019, **133**: 96–101.

[8] Wang GC, Liang JP, Wang Y, *et al*. Chemical constituents from *Flueggea virosa* [J]. *Chin J Nat Med*, 2008, **6**(4): 251–253.

[9] Liu YP, Chen A, Qiao L, *et al*. Studies on the chemical constituents from stems and leaves of *Flueggea virosa* [J]. *Guangdong Huagong*, 2015, **42**(5): 12–13.

[10] Chirkin E, Atkatlian W, Poree FH. The *Securinega alkaloids* [J]. *Alkaloids*, 2015, **74**: 1–120.

[11] Wehlauch R, Gademann K. *Securinega* alkaloids: Complex structures, potent bioactivities, and efficient total syntheses [J]. *Asian J Org Chem*, 2017, **6**(9): 1146–1159.

[12] Wang GY, Wang AT, Zhao BX, *et al*. Norsecurinamines A and B, two norsecurinine-derived alkaloid dimers from the fruits of *Flueggea virosa* [J]. *Tetrahedron Lett*, 2016, **57**(34): 3810–3813.

[13] Wu ZL, Zhao BX, Huang XJ, *et al*. Suffrutines A and B: a pair of Z/E isomeric indolizidne alkaloids from the roots of *Flueggea suffruticosa* [J]. *Angew Chem Int Ed*, 2014, **53**(23): 5796–5799.

[14] Wu ZL, Huang XJ, Xu MT, *et al*. Flueggeacosines A-C, dimeric securinine-type alkaloid analogues with neuronal differentiation activities from *Flueggea suffruticosa* [J]. *Org Lett*, 2018, **20**(23): 7703–7707.

[15] Zhao BX, Wang Y, Li C, *et al*. Flueggedine, a novel axisymmetric indolizidine alkaloid dimer from *Flueggea virosa* [J]. *Tetrahedron Lett*, 2013, **54**(35): 4708–4711.

[16] Wolinski K, Hinton JF, Pulay P. Efficient implementation of the gauge-independent atomic orbital method for NMR chemical shift calculations [J]. *J Am Chem Soc*, 1990, **112**(23): 8251–8260.

[17] Smith SG, Goodman JM. Assigning stereochemistry to single diastereoisomers by GIAO NMR calculation: The DP4 probability [J]. *J Am Chem Soc*, 2010, **132**(37): 12946–12959.

[18] Khuzhaev VU, Aripova SF, Abdullaev UA. Alkaloids of *Arundo donax*. IV. Donaxanine-A new pyrrolidine alkaloid from *Arundo donax* [J]. *Khim Prir Soedin*, 1995(5): 728–730.

[19] Ghosal S, Mazumder UK, Bhattacharya SK, *et al*. Chemical and pharmacological evaluation of *Banistereopsis argentea* Spring ex Juss [J]. *J Pharm Sci*, 1971, **60**(8): 1209–1212.

[20] Doe de Maindreville M, Levy J, Tillequin F, *et al*. Synthesis of borrerine [J]. *J Nat Prod*, 1983, **46**(3): 310–313.

[21] Aati HY, El-Gamal AA, Kayser O, *et al*. The phytochemical and biological investigation of *Jatropha pelargoniifolia* root native to the Kingdom of Saudi Arabia [J]. *Molecules*, 2018, **23**(8): 1892/1–1892/13.

[22] Gan N, Li T, Yang X, *et al*. Constituents in *Desmodium blandum* and their antitumor activities [J]. *Chin Tradit Herb Drugs*, 2009, **40**(6): 852–856.

[23] Shaaban KA, Shaaban M, Rahman H, *et al*. Karamomycins A-C: 2-Naphthalen-2-yl-thiazoles from *Nonomuraea endophytica* [J]. *J Nat Prod*, 2019, **82**(4): 870–877.

[24] Ouyang Y, Mitsunaga K, Koike K, *et al*. Alkaloids and quassinoids of *Brucea mollis* var. *tonkinesis* [J]. *Phytochemistry*, 1995, **39**(4): 911–913.

[25] Bahceevli AK, Kurucu S, Kolak U, *et al*. Alkaloids and aromatics of *Cyathobasis fruticulosa* (Bunge) Aellen [J]. *J Nat Prod*, 2005, **68**(6): 956–958.

[26] Verpoorte R, Joosse FT, Groenink H, *et al*. Alkaloids from *Strychnos floribunda* [J]. *Planta Med*, 1981, **42**(1): 32–36.

[27] Sun P, Zhang S, Li Y, *et al*. Harmine mediated neuroprotection via evaluation of glutamate transporter 1 in a rat model of global cerebral ischemia [J]. *Neurosci Lett*, 2014, **583**: 32–36.

[28] Chen D, Su A, Fu Y, *et al*. Harmine blocks herpes simplex virus infection through downregulating cellular NF-κB and MAPK pathways induced by oxidative stress [J]. *Antivir Res*, 2015, **123**: 27–38.

[29] Frisch MJ, Trucks GW, Schlegel HB, *et al*. *Gaussian 09, Revision A.02* [M]. Gaussian, Inc., Wallingford CT, 2009.

[30] Bruhn T, Schaumlöffel A, Hemberger Y, *et al*. *SpecDis Version 1.71* [M]. Berlin, 2017.

Cite this article as: XIE Qiu-Jie, ZHANG Wei-Yan, WU Zhen-Long, XU Ming-Tao, HE Qi-Fang, HUANG Xiao-Jun, CHE Chun-Tao, WANG Ying, YE Wen-Cai. Alkaloid constituents from the fruits of *Flueggea virosa* [J]. *Chin J Nat Med*, 2020, **18**(5): 385-392.